Anwar et al., *BioImpacts*. 2025;15:30257
doi: 10.34172/bi.30257
https://bi.tbzmed.ac.ir/

# Sustained release microneedle patch for pronounced systemic delivery of doxazosin mesylate

**Imran Anwar[1], Nadiah Zafar[2*], Asif Mahmood[3], Zulcaif[4*], Riffat Latif[5]**

[1]Faculty of Pharmacy, The University Lahore, Lahore, Pakistan
[2]Department of Pharmaceutics, Faculty of Pharmacy, Universiti Teknologi MARA Selangor, Puncak Alam Campus, Bandar Puncak Alam, Malaysia
[3]Department of Pharmacy, University of Chakwal, Chakwal, Pakistan
[4]Riphah Institute of Pharmaceutical Sciences (RIPS), Riphah International University, Lahore Campus, Lahore, Pakistan
[5]Avera Health and Science, Department of Pharmaceutical Sciences, South Dakota State University, United States

**Article Info**

***Article Type:***
Original Article

***Article History:***
Received: 6 Jan. 2024
Revised: 11 Apr. 2024
Accepted: 30 Apr. 2024
ePublished: 3 Aug. 2024

***Keywords:***
Microneedle patches
Transdermal delivery
Polyvinyl alcohol
Chitosan
Doxazosin mesylate

**Abstract**

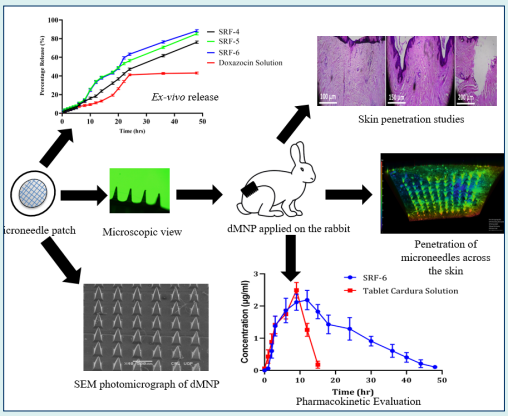


***Introduction:*** Microneedle patch is one of the fascinating drug delivery approaches that offers low invasiveness and a painless physical application to enhance the delivery of micro and macro-molecules into the skin.

***Methods:*** Variable contents of chitosan and polyvinyl alcohol were used for the development of doxazosin mesylate containing sustained release microneedle patches via solvent casting technique. The prepared patches were evaluated for microscopic evaluation, mechanical strength, drug loading (%) and Fourier transform infrared spectroscopy (FTIR) etc. The skin penetration study was performed by using pig ear skin and results were captured through confocal microscopy. *Ex-vivo* release study and pharmacokinetic evaluation were also performed.

***Results:*** Sharp needle tips with a height of 600µm and a base of 200µm were confirmed through microscopic examination. Optimized formulation (SRF-6) exhibited loading of 92.11% doxazosin mesylate with appreciable strength up to 1.94N force. *Ex-vivo* release studies revealed 87.24% release within 48 hours. Moreover, the pharmacokinetic parameters in case of optimized patch formulation (SRF-6) were markedly improved i.e. MRT (19.46 h), AUC (57.12 µg.h /mL), $C_{max}$ (2.16 µg /mL), $t_{max}$ (10.10 h) and $t_{1/2}$ (6.32 h) as compared to commercially available tablet. Biocompatibility of the developed patches was validated from skin irritation studies.

***Conclusion:*** Results confirmed the successful fabrication of microneedle patch having sufficient strength and effective penetration ability into the skin to ensure controlled release of incorporated drug for the intended duration. It can be employed as an efficient carrier system for other therapeutics those are prone to bioavailability issues due to first pass effect after their oral administration.

## Introduction

Drugs can be immediately and completely delivered into the bloodstream via a variety of approaches, including intramuscular (IM) and intravenous (IV), which guarantees a prompt therapeutic response.[1-3] Parenteral medication delivery have certain drawbacks like pain associated drug delivery leading to patient non-compliance and requirement of skilled staff.[4] Innovative and safer techniques such as mucosal administration,[5,6] magnetically modulated drug delivery systems,[7-9] nanofibers,[10] inhalers, and transdermal drug delivery systems (TDDS) have been developed and exercised to overcome aforementioned shortcomings.[11-13]

The transport of molecules with a large molecular weight

*Corresponding authors: Nadiah Zafar, Email: nadiahnoor99@gmail.com and Zulcaif, Email: zulcaifa@gmail.com

is a challenging task while dealing with skin barriers.[14,15] To address this issue, advancements have been made in the field of drug delivery. Techniques such as iontophoresis, sonophoresis, use of chemical enhancers, microneedle patches etc. have been introduced in literature to meet this challenge.[16-19]

Microneedles are one of the attractive TDDS and belong to the 3rd generation of TDDS. Microneedle patches (MNPs) consist of micron-scale needles that enable the direct administration of drugs into the blood stream. This self-contained and discrete dosage form has a number of advantages including controlled delivery, self-convenience, enhanced patient compliance and offer optimal bioavailability of drugs by bypassing the first-pass effect.[12,20-23] These are simple, cheap and can be developed as solid or hollow needles with length ranging from 50-900 µm. MNPs can be easily utilized for the delivery of protein, vaccine, insulin, and other drugs. A number of techniques are prevailing in literature to prepare such carrier systems like solvent casting, reactive ion etching, wet chemical etching, and solvent washing. A variety of natural, synthetic, biocompatible and biodegradable polymers have already been used as the basic materials involving solvent casting approach.[3,24-26] In literature a number of polymers like polyvinyl alcohol (PVA), carboxymethyl cellulose (CMC), hydroxypropyl methylcellulose (HPMC), chitosan (CS), thiolated chitosan (TC), alginic acid, Eudragit, and polyvinylpyrrolidone (PVP) have been tried for the development of dissolvable microneedle patches (dMNPs).[27-29]

CS is a biodegradable, non-toxic, biocompatible and semi-crystalline polymer obtained through the deacetylation of chitin using sodium hydroxide.[30-32] PVA is an aqueous-soluble and biodegradable polymer that demonstrates superior properties in dMNPs formulations. The mechanical characteristics, drug loading efficiency (%), and release behavior of dMNPs are majorly affected by the choice of polymer, making it an essential step in the process.[33-35]

Doxazosin mesylate is a quinazoline derivative having molecular formula $C_{24}H_{29}N_5O_8S$ and molecular weight of 547.6g /mL. It is lipophilic in nature. The log P value of doxazosin is 2.5. At the post-synaptic receptor, it acts as a competitive alpha1-antagonist. By competitively inhibiting post-synaptic alpha1-adrenergic receptors, doxazosin mesylate causes veins and arterioles to dilate, lowering blood pressure and total peripheral resistance. Oral bioavailability of doxazosin mesylate is 65% due to its first-pass effect. Although doses of 2 to 12 mg/day have been recommended in the treatment of benign prostatic hyperplasia (BPH). A dose of 4 mg/day is generally effective in most of the patients. Starting the treatment with 1 mg/day and titrating up every 1 to 2 weeks is the recommended course of action. It is classified as BCS class II and has a plasma half-life of 9 -12 hours. Commercially, doxazosin mesylate tablets are available in four different strengths like 1 mg, 2 mg, 4 mg, and 8 mg. The low bioavailability associated with oral delivery of this active therapeutic agent can be improved by avoiding the first pass effect or by delivering it through microneedle patch which further enhance the patient compliance.[36-40]

In our study, we developed and characterized the doxazosin mesylate containing sustained release dissolvable microneedle patch formulations having variable increments of polymers (chitosan and PVA). This innovative patch not only showcases ample strength and efficient penetration but also warrants the controlled release of drug over the designated time period. Additionally, our results have also confirmed improved pharmacokinetic profile in case of dMNPs as compared to the presently marketed tablet.

## Materials and Methods

### *Materials*

Chitosan low molecular weight (50 000-190 000 Da), Polyvinyl alcohol (99%) hydrolyzed (85 000-124 000) and acetic acid were procured from Sigma Aldrich (Germany). Doxazosin mesylate was generously gifted by Wilshire Laboratories (PVT), Pakistan. Silicon mold (array size = 10x10, height = 600µm and pitch = 500µm) was purchased from Micropoint technology, Singapore. Distilled water was taken from research laboratory of Faculty of Pharmacy, The University of Lahore.

### *Methods*

#### *Development of dissolvable microneedle patch*

Initially, different polymeric solutions alone and in combination as mentioned in Table 1 were prepared. A 1% acetic acid solution was used to ensure complete dissolution of chitosan solution. This mixture underwent continuous stirring on a magnetic stirrer at 37°C for a duration of 3 hours, and it was labelled as solution A. Simultaneously, 5% polyvinyl alcohol solution was prepared by dissolving required quantity of PVA in distilled water under constant stirring on a magnetic stirrer and labelled as solution B. Subsequently, to prepare polymeric blend, solution B was carefully transferred into solution A dropwise under continuous stirring for 30 minutes on

**Table 1.** Composition of microneedle patch formulations (SRF-1 to SRF-8)

| Formulation code | Chitosan (w/w%) | PVA (w/w%) | Doxazosin (mg/mL) |
|---|---|---|---|
| SRF-1 | 1 | - | 8 |
| SRF-2 | 1 | 5 | 8 |
| SRF-3 | 1.5 | - | 8 |
| SRF-4 | 1.5 | 5 | 8 |
| SRF-5 | 2 | - | 8 |
| SRF-6 | 2 | 5 | 8 |
| SRF-7 | 2.5 | - | 8 |
| SRF-8 | 2.5 | 5 | 8 |

hot plate magnetic stirrer, resulting in the formation of a homogeneous solution. Doxazosin mesylate was mixed in ethanol at a concentration of 8mg /mL and designated as solution C. Solution C was then gently introduced into the homogeneous solution and stirred for an additional 30 minutes. To load the drug effectively, the resulting homogeneous drug containing solution was poured onto a silicon mold and centrifuged for 3 hours at 5000 rpm. Following centrifugation, the solution was subjected to sonication for 1 hour. The drying was carried out at 45°C for 10 hours in hot air oven. Later on, the microneedle patch was carefully peeled off and stored in aluminum wrap for further characterization.

## Characterization

### Microscopic evaluation

The physical appearance and distribution pattern of microneedle tips in three selected formulations (SRF-4, SRF-5 and SRF-6) were evaluated using a light microscope (Nikon E200, Tokyo, Japan).[41] A scanning electron microscope (SEM) (NOVA Nano SEM 450, FEI, USA) was used to examine the surface morphology (shape, size, base, and pitch) of the microneedle patches at different magnification levels. SEM photomicrographs explored valuable insights into their physical attributes and structural properties.[42]

### Patch thickness, tensile strength and percentage elongation

A digital micrometer (Mitutoyo, Japan) was used to determine the thickness of the three dissolving microneedle patches (SRF-4, SRF-5, and SRF-6) those were chosen. Each patch was measured three times from different locations, and the average thickness was computed.[43] Tensile strength and percentage elongation were determined with universal tensile tester.

### Mechanical strength

To validate mechanical strength of developed microneedle patches (SRF-4, SRF-5 and SRF-6) skin penetration studies were performed, Universal testing machine (Testometric, UK) was used to conduct a compression test. The shape of the microneedles was noted and the dMNPs patches were visually examined under a light microscope (Nikon E200, Tokyo, Japan) prior to testing. This served as a reference for comparison with the post-compression test morphology, which would reveal any changes or breakage of the microneedles. The prepared patches were carefully fixed on metal platform of the testing machine's probe in a descending orientation for the compression test. After that, the probe was lowered at an average speed of 0.5 mm/s while exerting a force at a rate of 0.02 N per 30 seconds in order to make contact between the microneedles and the platform. After that, the probe was raised at the same pace. The microneedles were again examined under the light microscope after the test to assess their morphology, particularly any variation in sharpness, bending, or breakage. This analysis confirmed the mechanical strength of the dMNPs and their suitability for skin penetration without compromising their structural integrity.

## Penetration studies

### Histology study

The purpose of this study was to observe any histological alterations that might arise after applying the prepared patch onto the rabbit skin from dorsum region. Using a surgical blade (Feather, Japan), the skin lipids were gently removed. To give mechanical support, the skin was then placed on filter paper that had been previously soaked with phosphate buffer (pH 7.4). The dorsum was divided into two sides, with one side serving as a control and the other as the treated area where the dissolving microneedle patches were gently pressed onto the stratum corneum side for 1 minute. Following application, the dMNPs underwent staining procedures to assess and contrast their overall morphology with that of the control samples. The hematoxylin and eosin staining technique was used to separately stain the control and treated skin sections.[44]

### Confocal microscopy

Ear skin of the pig was taken and prepared microneedle patch was applied on it with the help of an applicator. After 1 minute of the application, skin was examined under confocal microscope. It offers insights into the structure and characteristics of these patches at microscopic level. It uses a pinhole to eliminate out-of-focus light, allowing only the light originating from the focal plane to reach the detector. This result in improved resolution and contrast compared to traditional wide-field microscopy. Microneedle patch treated skin was prepared for imaging by fixing them onto a glass slide and placed under same focal plane. A detailed, high-resolution image of the microneedle patch was captured.

### Drug loading (%)

Microneedles were carefully removed from the base plate using a sterile surgical blade (Feather Safety Razor Co., Ltd., Japan) under an optical microscope, the drug concentration in these microneedles was ascertained with great care. After that, the detached microneedles were vortexed and ultra-sonicated for 30 minutes in a solution mixture of acetonitrile and phosphate buffer (65:45). The samples were analyzed on High-Performance Liquid Chromatography (HPLC) after filtration to determine drug contents. Additionally, blank microneedles were also processed similarly and marked as control in current study. This rigorous approach allowed precise determination of the drug content successfully loaded within the microneedle patches and their comparison with the control samples.

### Fourier transform infrared spectroscopy

Fourier transform infrared spectroscopy (FTIR) analysis is frequently conducted to confirm complex formation, compatibility of the ingredients, and presence of

functional groups and their positioning in pure and patch state. This investigation was carried out using a FTIR Spectrophotometer (ATR-FTIR, Bruker, USA) and FTIR scans were captured for neat ingredients as well as developed drug-loaded dissolving microneedle patch at a scanning range of 400–4000 $cm^{-1}$. Individual component's IR spectra and the drug-loaded microneedle patches, were then compared in order to confirm possible chemical interactions, chemical composition, and structural changes those arise due to development of new formulations.[43,45,46]

### *Ex-vivo drug release study*

A Franz diffusion cell with a receptor compartment volume of 7.5 ml and a diffusion area of 2.5 $cm^{-2}$ was used to perform the *ex-vivo* release studies. The stratum corneum side of the rat skin was placed between the receptor and donor compartments of the Franz diffusion cell. The skin was covered in distinct layers for the experiment using the dissolved microneedle patches (SRF-4, SRF-5, and SRF-6) and the prepared doxazosin mesylate solution, separately. The Franz cell's receptor compartment was filled with phosphate buffer (pH 7.4). To ensure uniform experimental conditions and smooth conduct of experiment, the entire assembly was kept at a consistent temperature of 37 ± 1°C using a hot plate magnetic stirrer. Samples (0.5 ml) were taken out of the receptor compartment at predetermined intervals. To maintain the sink conditions, an equivalent volume of pH 7.4 phosphate buffer was added to the receiving compartment after each sampling event. HPLC method was used to determine the amount of doxazosin mesylate in each sample withdrawn after a particular time period thus validating the drug release behavior from the dissolving microneedle patches.

Each Franz cell's skin was meticulously removed after 48 hours. To guarantee homogeneity, each skin sample was then homogenized separately using a tissue homogenizer. Three distinct 100 ml beakers were filled with the homogenized skin samples, then ethanol was added to each beaker. In order to remove doxazosin mesylate from the skin, the combinations were allowed to soak and stir for the entire night. Subsequently, a 0.45µm syringe filter was used to filter the extract recovered from every beaker in order to exclude any particles or contaminants. The amount of doxazosin mesylate released from the dMNPs during the specified time periods was then measured by HPLC analysis of the filtered samples. Important information about the drug release behavior of the dissolving microneedle patches and their capacity to distribute doxazosin mesylate in a regulated and sustained way was obtained through this analysis process.[47]

## *In-vivo studies*

### *Pharmacokinetic evaluation*

The quantification of doxazosin mesylate in plasma samples was performed using a developed HPLC method from literature with slight modifications.[40] Chromatographic analysis was performed using a Shimadzu HPLC system with a DAD detector and a C-18 column (5µ x 4.6 mm x 250 mm). Acetonitrile and phosphate buffer were combined in a 65:45 ratio, respectively and employed as mobile phase. A small amount of orthophosphoric acid was added to adjust the pH i.e. 7.4. The samples were analyzed at $\boldsymbol{\lambda}_{max} = 238$ nm while the apparatus was operated at a flow rate of 1 ml/min. In all, eighteen albino rabbits weighing between two and three kilograms were subjected to current investigation. For seven days, the rabbits were acclimatized with the area conditions by their exposure to repetitive light and dark cycles. A crossover study design was used, and the rabbits were grouped into three groups (n = 6): Group A (Control), group B (treated with a marketed tablet Cardura 2 mg), and group C (treated with doxazosin mesylate-loaded microneedle patch). The rabbits were fasted for 12 hours before the administration research treatment with free access to water. Blood samples (3-4 ml) were withdrawn from the rabbits' jugular veins at pre-defined time intervals up to 24 hours. The plasma was separated from the blood samples using centrifugation operated at 5000 rpm for 10 minutes after the sample collection in EDTA tubes. One milliliter of plasma was deproteinized for measurement by adding an equivalent volume of methanol of HPLC grade as a protein precipitant. The mixture was centrifuged for 15 minutes to extract the plasma proteins after being vortexed for 3 minutes. After meticulous collection, the supernatant was injected into the HPLC system for analysis.

Group B was given dMNPs containing 8 mg of doxazosin mesylate after a two-week washout period, while Group C was given the commercially available tablet Cardura equivalent to 8 mg. In accordance with the specifications of the crossover study design, the entire process was repeated. $C_{max}$, $t_{max}$, $AUC_{0-t}$, Vd, AUM, $AUC_{0-\infty}$, and $t_{1/2}$ were calculated utilizing an Excel Adds-in tool pK solver. This comprehensive analysis provided valuable information on the pharmacokinetic parameters of doxazosin mesylate delivered through sustained-release dissolving microneedle patch (SRF-6).

### *Skin irritation study*

Using Draize scoring method, a microneedle patch containing doxazosin mesylate was applied on to rabbit skin to determine whether any sign of erythema or edema was present or not. The dorsal surface of the rabbit's skin was prepared for application of the patch after shaving, cleaning with phosphate buffer at pH 7.4, and cutting the hairs with an electrical trimming machine (Kemei, China). The experiment involved applying the optimized 3patches with microneedles having a homogeneous surface, regular geometry, and distinct sharpness (Fig. 2A and 2B). Notably, these selected dMNPs displayed transparent

properties along with sharp needles in each of them. In contrast, the remaining formulations did not show any distinct needle structures.

SEM analysis was carried out to examine the topography, uniform distribution, and dimensions of the microneedles in the prepared microneedle patch. The optimized polymeric microneedle patch (SRF-6) showed smooth surfaces, pyramid-shaped microneedles with sharp ends, and well-defined microneedles, as shown in Fig. 2C. The successful development of the dMNPs was confirmed from Fig. 2D that each individual needle possessed an intact structure with a height of 600 µm and base width of 200 µm. Pitch, or the space between needles, was measured to be 500 µm. Any slight decrease in dimensions was related with evaporation of solvent content during drying process thereby leading to hardness and slight shrinkage of developed microneedle array pattern.[4] These measurements suggested that the microneedles can facilitate transport of drugs through the skin in an effective manner.

### *Patch thickness, tensile strength and percentage elongation*

The thickness of the patch was observed to be directly influenced by the concentration of polymers. This thickness plays a crucial role in determining the patch's mechanical properties as well as distribution of the drug throughout the patch. To ensure accuracy, measurements were taken from various points within individual patches, and it was noticed that the thickness remained same in all areas. The mean thickness of the chosen samples (SRF-4, SRF-5, and SRF-6) was determined using the optical microscopy data. The measured values were 38.98µm, 41.54µm, and 51.22µm for SRF-4, SRF-5 and SRF-6, respectively as shown in Table 2. After careful evaluation of the thickness results, formulation SRF-6 was declared as the best formulation among the all developed formulations. It showed consistent drug loading, uniform distribution, no content loss during the manufacturing process and exhibited excellent mechanical strength.

In order to assess the mechanical characteristics of the developed patches, two essential parameters, namely elongation (%) and strength, were also measured. The percentage elongation provided a confirmation of the elastic nature exhibited by the microneedle patches (SRF-4, SRF-5 and SRF-6). Notably, formulations with higher elongation displayed significant elasticity. The average tensile strength (measured in mPa) for formulations SRF-4, SRF-5 and SRF-6 were found to be 0.38mPa, 0.39mPa, and 0.46mPa, respectively. Additionally, the average elongations (%) for the same formulations were recorded as 27.42%, 29.87%, and 32.98%, respectively (as shown in Table 2). Among these three formulations, SRF-6 demonstrated the most favorable tensile strength and elongation (%) due to optimal PVA contents in combination with chitosan. This rise in elongation was related with molecular interactions existing between PVA and chitosan via hydrogen bonding leading to rise in tensile strength and for the formation of a compact and rigid polymeric network structure.[50]

### *Mechanical Strength*

The mechanical strength of the prepared microneedle patches (SRF-4, SRF-5 and SRF-6) was measured through compression tests in order to confirm the integrity and stability during skin penetration of the developed patch formulations and the resilience of their needles. The average mechanical strength of formulations SRF-4, SRF-5 and SRF-6 was measured to be as 0.89N, 1.23N, and 1.94N, respectively, as depicted in Table 2. A force required to break usually greater than 0.21N guarantees adequate insertion of microneedles into the skin. Among these three formulations, SRF-6 displayed the most optimal mechanical strength. Notably, as the amount of

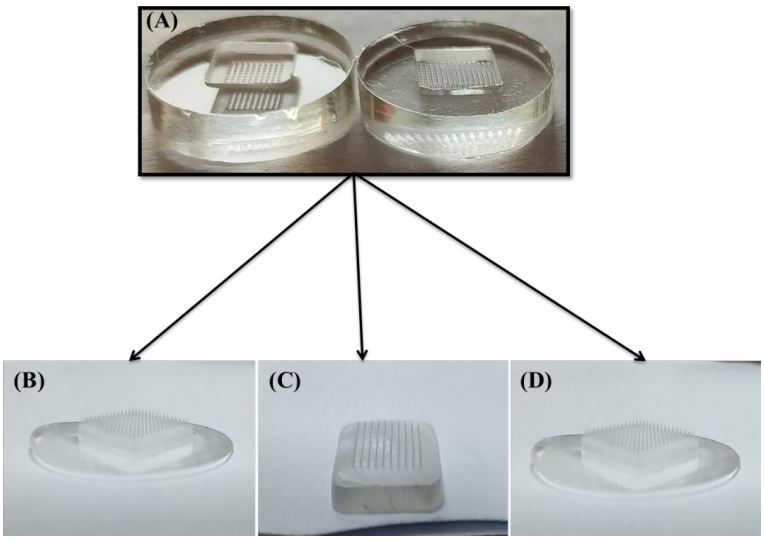


**Fig. 1.** Developed sustained release microneedle patches, A) molds, B) SRF-4, C) SRF-5 and D) SRF-6.

polymers increased, the force required to fracture the needles also increased because of the resistance offered by higher crosslinking (due to –OH and $–NH_2$ groups) between the incorporated polymers.[4]

Our results align with the findings of mechanical strength parameter in a study conducted by Dathathri et al.[51]

### *Penetration study*

Experiments involving histopathological analysis and microneedle patch's capability to penetrate rat skin were conducted. Followed by the application of patch on to the skin, the effects of different pressure intervals (30 seconds and 1 minute) were also recorded. Histopathological analysis was performed before the application of patch thereby exhibiting superficial dermis with no holes or invagination (Fig. 3A). Nevertheless, invaginations were seen after 30 seconds of pressure, suggesting that the microneedle patch had come into contact with the superficial dermis (Fig. 3B). Conversely, as the pressure grew, skin ruptured (Fig. 3C). This was further supported by microscopic observation of the visible holes following H & E staining (Fig. 3A-C). Furthermore, as seen in Fig. 3D, the confocal microscopy results verified the penetration of microneedles through the pig skin's subcutaneous layer and reach the dermis.

### *Drug loading (%)*

HPLC method was utilized to determine the amount of doxazosin mesylate loaded into the needles of microneedle patches. The loading efficiency of doxazosin mesylate within the needles of SRF-4, SRF-5 and SRF-6 was found to be 88.42%, 91.37% and 92.11%, respectively. These results validated the pharmaceutical application of these patches in drug delivery, reliance on technique of microneedle patch production, stability and excellent content uniformity of doxazosin mesylate. Furthermore, by changing the amount of doxazosin mesylate in the drug stock solution, the loading efficiency can be modulated. This flexibility in loading efficiency provides a valuable opportunity to optimize the drug dosage and tailor the formulation according to specific requirements. Overall, the high loading efficiency and the ability to hold appropriate drug quantity make the developed dMNPs a promising carrier for efficient drug delivery and offer potential benefits in various pharmaceutical applications.

### *Fourier transform infrared spectroscopy*

FTIR analysis was conducted to assess the compatibility of the formulation ingredients, identify potential complex formations, and confirm the presence of functional groups. The characteristic peaks in the FTIR spectrum of chitosan were located at 3342.03 $cm^{-1}$ and 2989.12 $cm^{-1}$ corresponding to –OH and –NH stretching, respectively. The FTIR spectrum of PVA was recorded and presented in Fig. 4. Notable features in the spectrum include a broadband at 3166.54 $cm^{-1}$, corresponding to the stretching movement of the hydroxyl group. The peak at 2952.48 $cm^{-1}$ indicates –CH stretching vibrations from the alkyl group, while the peak at 1417.42 $cm^{-1}$ indicates –OH group deformation. Additionally, peaks observed between 1554.34 $cm^{-1}$ and 1751.04 $cm^{-1}$ correspond to carbonyl (C=O) and C-O stretching, respectively.

Doxazosin mesylate displayed distinct peaks attributed to N-H stretching at 3371 $cm^{-1}$ and C=O stretching at 1597 $cm^{-1}$. The IR spectrum of the pure drug closely

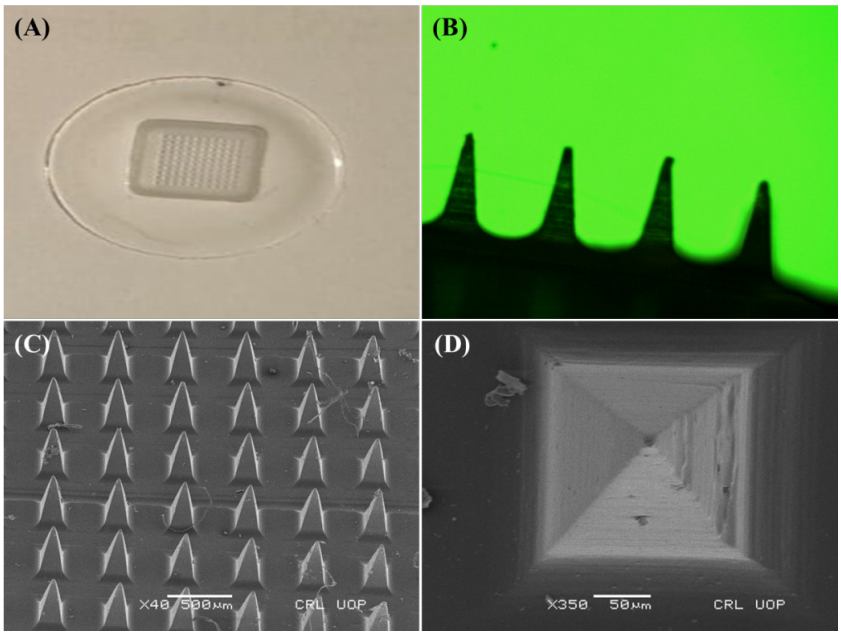


**Fig. 2.** Microneedles patch, A) macroscopic Ariel view, B) microscopic side view, C) SEM photomicrographs of microneedle patch at different magnification powers at x40 (Side view) and D) x350 (Arial view).

**Table 2.** Mechanical parameters of developed patches (SRF-4 to SRF-6)

| Parameters | SRF-4 | SRF-5 | SRF-6 |
|---|---|---|---|
| Thickness (µm) | 38.98 | 41.54 | 51.22 |
| Tensile strength (mPa) | 0.38 | 0.39 | 0.46 |
| Elongation (%) | 27.42 | 29.87 | 32.98 |
| Mechanical Strength (N) | 0.89 | 1.23 | 1.94 |

matched the reference standard IR spectrum of doxazosin mesylate, confirming the identity of the drug sample. The observed frequencies of functional groups in doxazosin mesylate were in agreement with the standard theoretical frequencies of these functional groups, providing further evidence for the drug's identity. The characteristic peaks of the pure drug sample are illustrated in the Fig. 4. When comparing the FTIR spectrum of the doxazosin mesylate loaded microneedle patch (SRF-6) to the IR spectrum of the pure ingredients, different peak patterns were discovered. With regard to doxazosin mesylate, the peak at 1597 $cm^{-1}$that was ascribed to C = O stretching moved to 1440 $cm^{-1}$. Furthermore, as seen in Fig. 4, the strength of the signal at 3371 $cm^{-1}$, which corresponds to N-H stretching, decreased. These changes in peak patterns indicate the interaction and incorporation of the drug into the microneedle formulation.

### *Ex-vivo drug release study*

The *ex-vivo* release of SRF-4, SRF-5, and SRF-6 was assessed via rabbit skin utilizing a Franz diffusion cell and phosphate buffer (pH 7.4). After administering similar quantities of doxazosin mesylate, the percentage of doxazosin mesylate that permeated through the rabbit skin was found to be 74.99% ± 1.25 (SRF-4), 84.11% ± 1.43 (SRF-5), and 87.24% ± 1.14 (SRF-6). In contrast, the doxazosin mesylate tablet solution showed a penetration of 42.11% ± 1.57 (Fig. 5C). These results confirmed that the SRF-6 formulation exhibited significantly higher drug permeation through the skin as compared to the other formulations and doxazosin mesylate solution. To determine the most suitable kinetic model for the release data, various models such as zero-order, first-order, Higuchi, and Korsmeyer Peppas were applied on release data using DD Solver Adds in Excel based software. After analyzing the results of formulation SRF-6, the regression coefficient ($R^2$) was found to be 0.977. Based on this high ($R^2$) value, the zero-order kinetic model was declared to be the best fit model for SRF-6 microneedle patch. Additionally, when the release data was analyzed using the Korsmeyer Peppas model, the $R^2$ value was 0.983, with value of "n" equal to 0.872. This confirmed that the mechanism of doxazosin mesylate release from microneedle patch was Super Case II release model. Super Case II release is associated with chain relaxation due to contact with water or dissolution media.

The quantification of doxazosin mesylate in the skin was performed by extracting the drug from the tissue. The analysis revealed that 2.45 ± 2.3% of doxazosin mesylate was present in the skin tissues when applied with SRF-6 microneedle patch. In contrast, only 1.27 ± 0.8% of doxazosin mesylate was found in the skin tissues when the drug was applied in solution form. These results indicated that the solution approach resulted in a lower percentage of doxazosin mesylate delivery to the skin, while the SRF-6 demonstrated good penetration and dissolution of the microneedles into the skin. This enhanced drug delivery efficiency of the patch can be attributed to the effective penetration of the microneedles, facilitating the drug release directly into the skin layers. Overall, the findings supported the superior performance of the selected patch formulation SRF-6 for efficient drug delivery to the skin compared to the traditional solution application method. The successful dissolution and penetration of the microneedles contribute to the improved drug uptake and bioavailability enhancement, making the patch a promising drug carrier for transdermal drug delivery. The comparison of the doxazosin tablet solution and patch was done to evaluate the bioavailability difference.

### *Pharmacokinetic evaluation*

#### *Standard curve*

Standard solutions of doxazosin mesylate were prepared by diluting the working stock solution across a range of concentrations from 10 µg /mL to 50 µg /mL. This included concentrations at 10 µg /mL, 20 µg /mL, 30 µg /mL, 40 µg /mL and 50 µg /mL. Each solution was injected into the HPLC system, and the resulting peak areas were recorded and tabulated. A plot was generated using this data, with concentrations on the X-axis and peak areas on the Y-axis, providing a visual representation of the relationship between concentration and peak area. From this plot, key parameters such as the correlation coefficient, y-intercept, and slope of the regression line were calculated to assess the linearity of the method and the relationship between analyte concentration and HPLC response. This process of preparing standard solutions, performing HPLC analysis, and calculating relevant parameters helps to validate the accuracy of the HPLC method for quantitatively analyzing doxazosin mesylate.

An *in-vivo* pharmacokinetic study was conducted using healthy rabbits to assess the sustained release potential of doxazosin mesylate loaded microneedle patch. The study was aimed to compare the pharmacokinetic profiles (including parameters such as $t_{max}$, $C_{max}$, $t_{1/2}$, AUC, MRT, and Vd) of SRF-6 with the commercially available tablet Cardura 2 mg. Doxazosin mesylate concentrations were measured from both the microneedle-loaded formulation and the Cardura 2 mg tablet at various time intervals. The plasma concentration versus time curve is illustrated in Fig. 5D. The maximum concentrations ($C_{max}$) of doxazosin mesylate released from the oral tablet solution

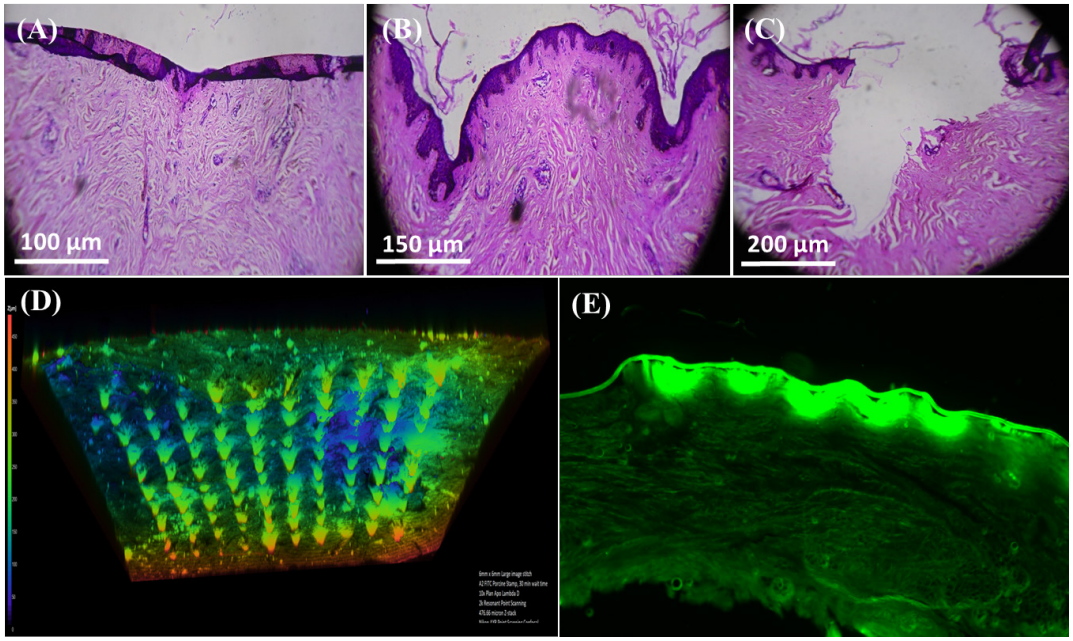


**Fig. 3.** Penetration study of sustained release microneedle patch (SRF-6), A) before application patch B) after application of patch for 30 sec, C) after application of patch for 1 minute, D) Confocal Microscopy image after application of patch and E) displaying drug penetrated across the stratum corneum.

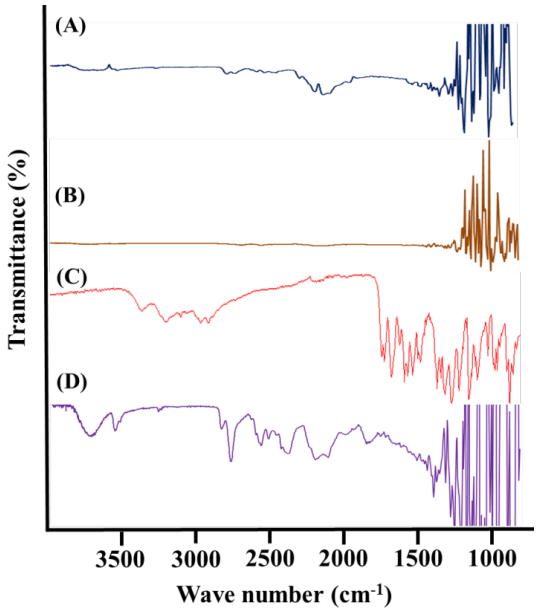


**Fig. 4.** FTIR spectrum, A) chitosan, B) polyvinyl alcohol, C) doxazosin mesylate, D) microneedle patch (SRF-6).

and microneedle patch were determined to be 0.95µg /mL and 2.16 µg /mL, respectively. The time to reach maximum plasma concentration ($t_{max}$) was observed at 2.67 hours for the tablet, indicating higher absorption. Conversely, the microneedle patch formulation exhibited a prolonged $t_{max}$ of 10.10 hours. The half-life ($t_{1/2}$) of doxazosin mesylate was 1.75 h for the Cardura 2mg tablet, which was extended to 6.32 h in case of doxazosin mesylate loaded dMNPs. The increased half-life suggested a slower release of the drug from the microneedle patch, resulting in a longer presence of the drug in the plasma and consequently contributing to enhanced bioavailability and sustained effects of doxazosin mesylate. Furthermore, the mean residence time (MRT) and area under the curve (AUC) for the Cardura 2mg tablet were 5.067 hours and 6.61 µg.h /mL, respectively, while for the microneedle patch formulation, these values were increased to 19.46 hours and 57.12 µg.h /mL, respectively. A notable disparity was observed in the pharmacokinetic profiles between the Cardura 2mg tablet and the developed doxazosin mesylate loaded sustained release microneedle patch. Consequently, the *in-vivo* evaluation of the optimized microneedle patch formulation demonstrated its capability to prolong the systemic availability of doxazosin mesylate, indicating its potential for sustained drug release and improved therapeutic outcomes. Improvement in pharmacokinetic parameters while comparing microneedle patch with the oral solution has already been reported in a study conducted by Habib et al.[43]

### *Skin irritation study*

The Draize scoring method was utilized to meticulously apply the microneedle patch to the rabbits' skin in order to evaluate any possible discomfort. The rabbit skin was rendered hairless prior to the implantation of the microneedle patch. The findings were made up to 48 h after application as well as at 0 hours. Upon the initial application of the dMNPs, slight erythema (reddening of the skin) was noted. This mild erythema could be attributed to the presence of a higher number of microneedles in the patch, causing minor pores on the skin. Nevertheless, there were no indications of edema, erythema, or skin allergies following the 48 h monitoring period. These findings imply that the formulated microneedle patch

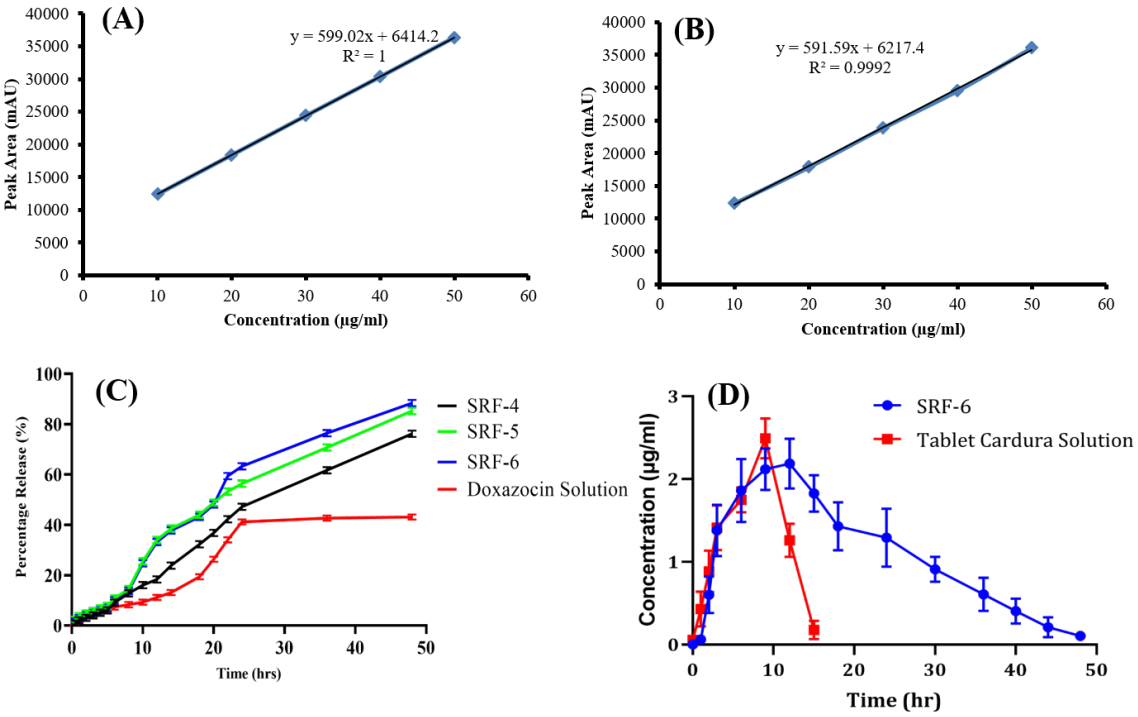


**Fig. 5.** A) Standard curve of doxazosin mesylate in mobile phase, B) Standard curve of doxazosin mesylate in rabbit plasma, C) *Ex-vivo* release study of prepared formulations and marketed tablet Cardura solution and D) *In-vivo* comparison of Plasma concentration vs time graph of sustained release microneedle patch and marketed tablet Cardura.

was non-toxic, non-irritant, and biocompatible.[52] The absence of adverse reactions on the skin indicates that the microneedle patch is well-tolerated and safe for skin applications.

## Conclusion

Our investigation into the utilization of a microneedle patch for systemic delivery of doxazosin mesylate has proven to be a promising and successful endeavor. The sustained-release microneedle patch, particularly the optimized SRF-6 variant, demonstrated notable attributes, including well-defined microscopic features, robust mechanical strength, and a high drug loading capacity. The *ex-vivo* release study provided evidence of the sustained and controlled release of doxazosin mesylate (87.24%) for 48 h. Furthermore, our pharmacokinetic evaluation revealed improved pharmacokinetic parameters in case of SRF-6 patch compared to the commercially available tablet.

In the pursuit of advancing microneedle patch technology for drug delivery, an exciting avenue lies in integrating cutting-edge smart technologies. By incorporating sensors and feedback mechanisms into microneedle patches, the potential to revolutionize personalized medicine emerges. Real-time monitoring of drug delivery parameters and patient response becomes feasible, offering unprecedented insights into treatment efficacy and patient-specific therapeutic needs. This transformative approach not only enhances the precision and efficiency of drug delivery but also fosters a deeper understanding of individual patient responses, paving the way for tailored therapeutic interventions leading to enhanced patient compliance and personalized treatment regimens.

### Authors Contribution

**Conceptualization:** Imran Anwar, Zulcaif.
**Data curation:** Zulcaif, Imran Anwar.
**Formal analysis:** Zulcaif, Asif Mahmood.
**Funding acquisition:** Nadiah Zafar.
**Investigation:** Imran Anwar.
**Methodology:** Nadiah Zafar, Zulcaif.
**Project administration:** Zulcaif, Asif Mahmood.
**Resources:** Imran Anwar, Nadiah Zafar.
**Software:** Zulcaif, Asif Mahmood.
**Supervision:** Nadiah Zafar, Zulcaif.
**Validation:** Asif mahmood, Riffat Latif.
**Visualization:** Zulcaif, Nadiah Zafar.

### Research Highlights

**What is the current knowledge?**

- Doxazosin, an alpha-1 blocker used to treat hypertension and urinary retention associated with drawback i.e. low bioavailability.

**What is new here?**

- Successful loading of doxazosin mesylate into the optimized dissolvable microneedle patches, bypassing the extensive first pass effect results in enhanced bioavailability.

**Writing–original draft:** Imran Anwar.
**Writing–review & editing:** Asif Mahmood, Riffat Latif.

## Competing Interests

The authors of this study affirm that they have no conflicts of interest to disclose.

## Data Availability Statement

For those interested in accessing the data presented in this study, requests can be directed to the corresponding author. We value transparency and collaboration in scientific research and are committed to sharing our findings with the broader scientific community.

## Ethical Statement

The animal study conducted as part of this research adhered to ethical guidelines and received approval from the Institutional Research Ethics Committee of the Faculty of Pharmacy, The University of Lahore. The approval reference number is IREC-2022-18.

## Funding

This research received no external funding.

## References

1. Manchanda S, Das N, Chandra A, Bandyopadhyay S, Chaurasia S. Fabrication of advanced parenteral drug-delivery systems. In: Tekade RK, ed. *Drug Delivery Systems*. Academic Press; **2020**. p. 47-84. doi: 10.1016/b978-0-12-814487-9.00002-8.
2. Ahmad Z, Khan MI, Siddique MI, Sarwar HS, Shahnaz G, Hussain SZ, et al. Fabrication and characterization of thiolated chitosan microneedle patch for transdermal delivery of tacrolimus. *AAPS PharmSciTech* **2020**; 21: 68. doi: 10.1208/s12249-019-1611-9.
3. Ahmad Z, Zafar N, Mahmood A, Sarfraz RM, Latif R, Gad HA. Fast dissolving microneedle patch for pronounced systemic delivery of an antihyperlipidemic drug. *Pharm Dev Technol* **2023**; 28: 896-906. doi: 10.1080/10837450.2023.2272863.
4. Khalid A, Shoaib Sarwar H, Sarfraz M, Farhan Sohail M, Jalil A, Bin Jardan YA, et al. Formulation and characterization of thiolated chitosan/polyvinyl acetate-based microneedle patch for transdermal delivery of dydrogesterone. *Saudi Pharm J* **2023**; 31: 669-77. doi: 10.1016/j.jsps.2023.03.007.
5. Thwala LN, Préat V, Csaba NS. Emerging delivery platforms for mucosal administration of biopharmaceuticals: a critical update on nasal, pulmonary and oral routes. *Expert Opin Drug Deliv* **2017**; 14: 23-36. doi: 10.1080/17425247.2016.1206074.
6. Sosnik A, das Neves J, Sarmento B. Mucoadhesive polymers in the design of nano-drug delivery systems for administration by non-parenteral routes: a review. *Prog Polym Sci* **2014**; 39: 2030-75. doi: 10.1016/j.progpolymsci.2014.07.010.
7. Aslam H, Shukrullah S, Naz MY, Fatima H, Hussain H, Ullah S, et al. Current and future perspectives of multifunctional magnetic nanoparticles based controlled drug delivery systems. *J Drug Deliv Sci Technol* **2022**; 67: 102946. doi: 10.1016/j.jddst.2021.102946.
8. Shrivastava P, Vishwakarma N, Gautam L, Vyas SP. Magnetically responsive polymeric gels and elastomeric system(s) for drug delivery. In: Vyas SP, Agrawal U, Sharma R, eds. *Smart Polymeric Nano-Constructs in Drug Delivery*. Academic Press; **2023**. p. 129-50. doi: 10.1016/b978-0-323-91248-8.00012-x.
9. Vinhas A, Almeida AF, Rodrigues MT, Gomes ME. Prospects of magnetically based approaches addressing inflammation in tendon tissues. *Adv Drug Deliv Rev* **2023**; 196: 114815. doi: 10.1016/j.addr.2023.114815.
10. Nadaf A, Gupta A, Hasan N, Fauziya, Ahmad S, Kesharwani P, et al. Recent update on electrospinning and electrospun nanofibers: current trends and their applications. *RSC Adv* **2022**; 12: 23808-28. doi: 10.1039/d2ra02864f.
11. Alkilani AZ, Nasereddin J, Hamed R, Nimrawi S, Hussein G, Abo-Zour H, et al. Beneath the skin: a review of current trends and future prospects of transdermal drug delivery systems. *Pharmaceutics* **2022**; 14: 1152. doi: 10.3390/pharmaceutics14061152.
12. Sabbagh F, Kim BS. Recent advances in polymeric transdermal drug delivery systems. *J Control Release* **2022**; 341: 132-46. doi: 10.1016/j.jconrel.2021.11.025.
13. Xie Y, He J, Li S, Chen X, Zhang T, Zhao Y, et al. A transdermal drug delivery system based on nucleic acid nanomaterials for skin photodamage treatment. *Adv Funct Mater* **2023**; 33: 2303580. doi: 10.1002/adfm.202303580.
14. Cheng T, Tai Z, Shen M, Li Y, Yu J, Wang J, et al. Advance and challenges in the treatment of skin diseases with the transdermal drug delivery system. *Pharmaceutics* **2023**; 15: 2165. doi: 10.3390/pharmaceutics15082165.
15. Phatale V, Vaiphei KK, Jha S, Patil D, Agrawal M, Alexander A. Overcoming skin barriers through advanced transdermal drug delivery approaches. *J Control Release* **2022**; 351: 361-80. doi: 10.1016/j.jconrel.2022.09.025.
16. Gao Y, Du L, Li Q, Li Q, Zhu L, Yang M, et al. How physical techniques improve the transdermal permeation of therapeutics: a review. *Medicine (Baltimore)* **2022**; 101: e29314. doi: 10.1097/md.0000000000029314.
17. Chakraborty R, Afrose N, Kuotsu K. Novel synergistic approaches of protein delivery through physical enhancement for transdermal microneedle drug delivery: a review. *J Drug Deliv Sci Technol* **2023**; 84: 104467. doi: 10.1016/j.jddst.2023.104467.
18. Dandekar AA, Garimella HT, German CL, Banga AK. Microneedle mediated iontophoretic delivery of tofacitinib citrate. *Pharm Res* **2023**; 40: 735-47. doi: 10.1007/s11095-022-03190-5.
19. Kumar V, Praveen N, Kewlani P, Arvind, Singh A, Gautam AK, et al. Transdermal drug delivery systems. In: Santra TS, Shinde AU, eds. *Advanced Drug Delivery: Methods and Applications*. Singapore: Springer; **2023**. p. 333-62. doi: 10.1007/978-981-99-6564-9_13.
20. Soni D, Prakash K, Shakeel K, Kesharawani P. Current trends and recent development of transdermal drug delivery system TDDS. *Asian J Pharm Res Dev* **2023**; 11: 181-9. doi: 10.22270/ajprd.v11i3.1274.
21. Gera AK, Burra RK. The rise of polymeric microneedles: recent developments, advances, challenges, and applications with regard to transdermal drug delivery. *J Funct Biomater* **2022**; 13: 81. doi: 10.3390/jfb13020081.
22. Zhang H, Pan Y, Hou Y, Li M, Deng J, Wang B, et al. Smart physical-based transdermal drug delivery system: towards intelligence and controlled release. *Small* **2024**; 20: e2306944. doi: 10.1002/smll.202306944.
23. Nazary Abrbekoh F, Salimi L, Saghati S, Amini H, Fathi Karkan S, Moharamzadeh K, et al. Application of microneedle patches for drug delivery; doorstep to novel therapies. *J Tissue Eng* **2022**; 13: 20417314221085390. doi: 10.1177/20417314221085390.
24. Andranilla RK, Anjani QK, Hartrianti P, Donnelly RF, Ramadon D. Fabrication of dissolving microneedles for transdermal delivery of protein and peptide drugs: polymer materials and solvent casting micromoulding method. *Pharm Dev Technol* **2023**; 28: 1016-31. doi: 10.1080/10837450.2023.2285498.
25. Bao L, Park J, Bonfante G, Kim B. Recent advances in porous microneedles: materials, fabrication, and transdermal applications. *Drug Deliv Transl Res* **2022**; 12: 395-414. doi: 10.1007/s13346-021-01045-x.
26. Zarei Chamgordani N, Asiaei S, Ghorbani-Bidkorpeh F, Babaee Foroutan M, Mahboubi A, Moghimi HR. Fabrication of controlled-release silver nanoparticle polylactic acid microneedles with long-lasting antibacterial activity using a micro-molding solvent-casting technique. *Drug Deliv Transl Res* **2024**; 14: 386-99. doi: 10.1007/s13346-023-01406-8.
27. Arshad J, Barkat K, Ashraf MU, Badshah SF, Ahmad Z, Anjum I, et al. Preparation and characterization of polymeric cross-linked hydrogel patch for topical delivery of gentamicin. *e-Polymers* **2023**; 23: 20230045. doi: 10.1515/epoly-2023-0045.
28. Oh NG, Hwang SY, Na YH. Fabrication of a PVA-based hydrogel microneedle patch. *ACS Omega* **2022**; 7: 25179-85. doi: 10.1021/acsomega.2c01993.

29. Xu N, Zhang M, Xu W, Ling G, Yu J, Zhang P. Swellable PVA/PVP hydrogel microneedle patches for the extraction of interstitial skin fluid toward minimally invasive monitoring of blood glucose level. *Analyst* **2022**; 147: 1478-91. doi: 10.1039/d1an02288a.
30. Ryall C, Chen S, Duarah S, Wen J. Chitosan-based microneedle arrays for dermal delivery of *Centella asiatica*. *Int J Pharm* **2022**; 627: 122221. doi: 10.1016/j.ijpharm.2022.122221.
31. Younas A, Dong Z, Hou Z, Asad M, Li M, Zhang N. A chitosan/fucoidan nanoparticle-loaded pullulan microneedle patch for differential drug release to promote wound healing. *Carbohydr Polym* **2023**; 306: 120593. doi: 10.1016/j.carbpol.2023.120593.
32. Yu X, Wang C, Wang Y, Li L, Gao X, Zhu T, et al. Microneedle array patch made of Kangfuxin/chitosan/fucoidan complex enables full-thickness wound healing. *Front Chem* **2022**; 10: 838920. doi: 10.3389/fchem.2022.838920.
33. Malek-Khatabi A, Rad-Malekshahi M, Shafiei M, Sharifi F, Motasadizadeh H, Ebrahiminejad V, et al. Botulinum toxin A dissolving microneedles for hyperhidrosis treatment: design, formulation and in vivo evaluation. *Biomater Sci* **2023**; 11: 7784-804. doi: 10.1039/d3bm01301d.
34. Weng J, Yang J, Wang W, Wen J, Fang M, Zheng G, et al. Application of microneedles combined with dendritic cell-targeted nanovaccine delivery system in percutaneous immunotherapy for triple-negative breast cancer. *Nanotechnology* **2023**; 34: 475101. doi: 10.1088/1361-6528/ace97b.
35. Hussain I, Muhammad N, Subhani Q, Shou D, Jin M, Yu L, et al. A review on structural aspects and applications of PAMAM dendrimers in analytical chemistry: frontiers from separation sciences to chemical sensor technologies. *TrAC Trends Anal Chem* **2022**; 157: 116810. doi: 10.1016/j.trac.2022.116810.
36. Mandić L, Ljubić I, Džeba I. Time-resolved spectroscopic and computational study of the initial events in doxazosin photochemistry. *Spectrochim Acta A Mol Biomol Spectrosc* **2024**; 306: 123595. doi: 10.1016/j.saa.2023.123595.
37. Yadav PS, Hajare AA, Patil KS. Development and validation of UV spectrophotometric method for doxazosin mesylate in bulk and tablets. *Res J Pharm Technol* **2022**; 15: 2675-80. doi: 10.52711/0974-360x.2022.00447.
38. Wahan SK, Sharma B, Chawla PA. Medicinal perspective of quinazolinone derivatives: recent developments and structure–activity relationship studies. *J Heterocycl Chem* **2022**; 59: 239-57. doi: 10.1002/jhet.4382.
39. Ding Y, Zhang N, Zhao J, Lv H, Wang X, Zhao B, et al. Determination of antihypertensive drugs irbesartan and doxazosin mesylate in healthcare products and urine samples using surface-enhanced Raman scattering. *Anal Bioanal Chem* **2022**; 414: 7813-22. doi: 10.1007/s00216-022-04315-w.
40. Hima P, Vageesh M, Tomasini M, Poater A, Dey R. Transition metal-free synthesis of 2-aryl quinazolines via alcohol dehydrogenation. *Mol Catal* **2023**; 542: 113110. doi: 10.1016/j.mcat.2023.113110.
41. Maurya A, Nanjappa SH, Honnavar S, Salwa M, Murthy SN. Rapidly dissolving microneedle patches for transdermal iron replenishment therapy. *J Pharm Sci* **2018**; 107: 1642-7. doi: 10.1016/j.xphs.2018.02.011.
42. Chen J, Wang M, Ye Y, Yang Z, Ruan Z, Jin N. Fabrication of sponge-forming microneedle patch for rapidly sampling interstitial fluid for analysis. *Biomed Microdevices* **2019**; 21: 63. doi: 10.1007/s10544-019-0413-x.
43. Habib R, Azad AK, Akhlaq M, Al-Joufi FA, Shahnaz G, Mohamed HR, et al. Thiolated chitosan microneedle patch of levosulpiride from fabrication, characterization to bioavailability enhancement approach. *Polymers (Basel)* **2022**; 14: 415. doi: 10.3390/polym14030415.
44. Li W, Terry RN, Tang J, Feng MR, Schwendeman SP, Prausnitz MR. Rapidly separable microneedle patch for the sustained release of a contraceptive. *Nat Biomed Eng* **2019**; 3: 220-9. doi: 10.1038/s41551-018-0337-4.
45. Ahmad Z, Khan MI, Siddique MI, Sarwar HS, Shahnaz G, Hussain SZ, et al. Fabrication and characterization of thiolated chitosan microneedle patch for transdermal delivery of tacrolimus. *AAPS PharmSciTech* **2020**; 21: 68. doi: 10.1208/s12249-019-1611-9.
46. Mahmood HS, Ghareeb MM, Hamzah ZO, Kadhim ZM. Formulation and characterization of flurbiprofen nanoparticles loaded microneedles. *Kerbala J Pharm Sci* **2021**; 1: 90-107. doi: 10.13140/rg.2.2.30099.55843.
47. Nguyen HX, Bozorg BD, Kim Y, Wieber A, Birk G, Lubda D, et al. Poly (vinyl alcohol) microneedles: fabrication, characterization, and application for transdermal drug delivery of doxorubicin. *Eur J Pharm Biopharm* **2018**; 129: 88-103. doi: 10.1016/j.ejpb.2018.05.017.
48. Hirobe S, Azukizawa H, Matsuo K, Zhai Y, Quan YS, Kamiyama F, et al. Development and clinical study of a self-dissolving microneedle patch for transcutaneous immunization device. *Pharm Res* **2013**; 30: 2664-74. doi: 10.1007/s11095-013-1092-6.
49. Alotaibi BS, Khan AK, Kharaba Z, Yasin H, Yasmin R, Ijaz M, et al. Development of poly(vinyl alcohol)-chitosan composite nanofibers for dual drug therapy of wounds. *ACS Omega* **2024**; 9: 12825-34. doi: 10.1021/acsomega.3c08856.
50. Zatalini DF, Hendradi E, Drake P, Sari R. The effect of chitosan and polyvinyl alcohol combination on physical characteristics and mechanical properties of chitosan-PVA-*Aloe vera* film. *J Farm Ilmu Kefarmasian Indones* **2023**; 10: 151-61. doi: 10.20473/jfiki.v10i22023.151-161.
51. Dathathri E, Lal S, Mittal M, Thakur G, De S. Fabrication of low-cost composite polymer-based micro needle patch for transdermal drug delivery. *Appl Nanosci* **2020**; 10: 371-7. doi: 10.1007/s13204-019-01190-3.
52. Fathi-Karkan S, Heidarzadeh M, Taghavi Narmi M, Mardi N, Amini H, Saghati S, et al. Exosome-loaded microneedle patches: promising factor delivery route. *Int J Biol Macromol* **2023**; 243: 125232. doi: 10.1016/j.ijbiomac.2023.125232.